International Journal of Thermophysics, Vol. 18, No. 3, 1997

An Integral Solution for Thermal Diffusion in Periodic Multilayer Materials: Application to Iron/Copper Multilayers

D. Josell,[1,2] A. Cezairliyan,[1] D. van Heerden,[1] and B. T. Murray[1]

Received May 7, 1996

A closed-form solution for heat transfer through a periodic multilayer material utilizing a transfer matrix technique is presented. The benefit of this technique for periodic multilayer samples is that the use of eigenvector decomposition significantly simplifies the solution. Experimental results, obtained in the vicinity of 1200 K on samples composed of 10 bilayers of nominally 2/3 μm copper and 4/3 μm iron on 75-μm molybdenum substrates, are presented.

KEY WORDS: copper; interfaces; iron; laser pulse heating; molybdenum; multilayer; thermal diffusivity; thermal pulse heating; thin films.

1. INTRODUCTION

Increased interest in multilayer materials in various applications, including thermal barrier coatings, has necessitated the development of techniques for measuring their properties. Thermal diffusivity (thermal conductivity divided by the product of specific heat and density) is one of the key transport properties. Methods for determining thermal diffusivity of relatively thick ($\sim$1-mm) monolithic samples constitute a mature field. Indeed, numerous materials have been studied at elevated temperatures by transient experiments utilizing surface thermal pulses [1, 2]. Studies of heat transfer in multilayer materials are less common, due partly to the difficulty of measurement on thin ($\sim$100-μm) samples. Theoretical treatments exist for heat transfer through the most general multilayers, each layer with independent thickness and thermal transport properties [3, 4]. These

[1] Metallurgy Division, National Institute of Standards and Technology, Gaithersburg, Maryland 20899, U.S.A.

[2] To whom correspondence should be addressed.

0195-928X/97/0500-0865$12.50/0

solutions range from separation of variable techniques [5] to recursion techniques [6]. The exact solution presented in this paper for heat transfer in periodic multilayers has computational complexity *independent* of the number of repeat units in the multilayer, i.e., the number of bilayers.

In thermal pulse experiments, a heat pulse is delivered to the front surface of a sample of known thickness that is being maintained in a constant ambient temperature, and the temperature of the rear, occasionally the front, surface of the sample is subsequently monitored. As the heat delivered by the pulse diffuses within the sample, the temperature of the front surface decreases and that of the rear surface increases. After sufficient time, the temperature of the entire sample decreases to the ambient temperature through radiative or conductive heat loss. It is through theoretical modeling of the *temperature transient* of either surface that the thermal diffusivity of the sample is determined. Analysis of experiments on multilayer samples has in the past [7, 8] been accomplished by discretizing the heat transfer equation and boundary conditions and time stepping forward to permit simulations of heat transfer through the sample. Though this technique does permit analysis of data, it requires a boundary condition to represent each interface in the material and the solutions typically yield little insight into the general behavior of the solution.

In this paper, a closed-form solution utilizing transfer matrices is presented. For periodic multilayer samples, the use of eigenvector decomposition significantly simplifies the solution. Measurements in the vicinity of 1200 K on samples composed of 10 bilayers of nominally 2/3 μm copper and 4/3 μm iron on 75 μm molybdenum substrates are presented, and the results are analyzed utilizing the developed theory.

2. THEORY

2.1. Solution of the Heat Transfer Equation

For one-dimensional heat flow, solutions utilizing heat flux and temperature transfer matrices can be found in the literature [9]. The transfer matrix relates the heat flux and temperature on both sides of a material. Where the heat flux through and temperature on surface n are of the form

$$Q_n^0(t) = Q_n(\omega)\, e^{i\omega t} \qquad \text{and} \qquad T_n^0(t) = T_n(\omega)\, e^{i\omega t} \tag{1}$$

as per the schematic diagram shown in Fig. 1, the heat flux and temperature on each side of the layer are related by

$$\begin{bmatrix} Q_0(\omega) \\ T_0(\omega) \end{bmatrix} = \begin{bmatrix} \tau_{11}(\omega) & \tau_{12}(\omega) \\ \tau_{21}(\omega) & \tau_{22}(\omega) \end{bmatrix} \begin{bmatrix} Q_1(\omega) \\ T_1(\omega) \end{bmatrix} \tag{2}$$

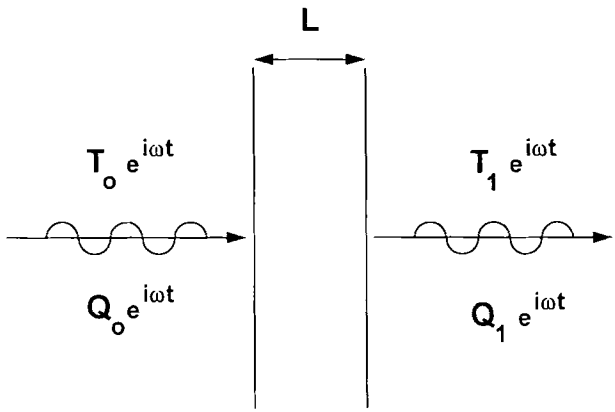

Fig. 1. Schematic diagram of a single layer indicating directions of positive heat flux Q on the surfaces.

The elements of the transfer matrix τ are evaluated using the thermal diffusion equation and heat flux boundary conditions to find

$$\begin{aligned} \tau_{11} &= \tau_{22} = \cosh\left(\sqrt{\frac{i\omega}{\alpha}}\, L\right) \\ \tau_{12}/(\kappa\sqrt{i\omega/\alpha}) &= \tau_{21}\kappa\sqrt{i\omega/\alpha} = \sinh\left(\sqrt{\frac{i\omega}{\alpha}}\, L\right) \end{aligned} \tag{3}$$

where α, κ, and L are the thermal diffusivity, thermal conductivity, and thickness, respectively, of the layer. The elements of the transfer matrix R for an interface, interface resistance ρ, are [9]

$$R_{11} = R_{22} = 1.0, \qquad R_{12} = 0, \qquad \text{and} \qquad R_{21} = \rho \tag{4}$$

The transfer matrix for a layered structure is the product of the transfer matrices of all the layers in the order in which they occur from front to rear in the sample. Thus, for the periodic multilayer composed of N repetitions of any basis structure, e.g., a layer of copper and a layer of iron, pictured schematically in Fig. 2, the transfer matrix M for the entire multilayer, in terms of the transfer matrices C_1, C_2, etc., of each of the N repetitions of the basis structure, is

$$M \equiv C_1 \cdot C_2 \cdot \cdots \cdot C_N = C^N \tag{5}$$

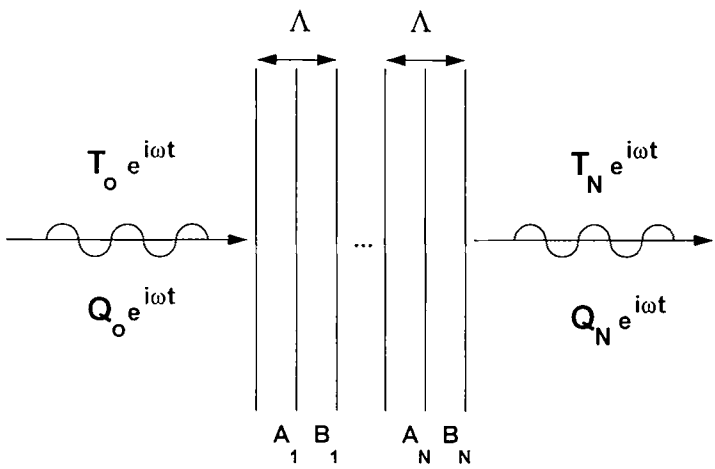

Fig. 2. Schematic diagram of a multilayer composed of N repetitions of a repeat unit, in this case a bilayer Λ thick composed of a layer of A followed by a layer of B. Each layer in the repeat unit has its own thickness, thermal diffusivity, and thermal conductivity. The interface resistance is associated with the planar interface where the layers of A and B meet.

where the last equality holds because the N transfer matrices are identical to the transfer matrix of the basis structure. The transfer matrix M defined above relates the heat flux and temperature for the front and rear surfaces of the multilayer sample according to

$$\begin{bmatrix} Q_0(\omega) \\ T_0(\omega) \end{bmatrix} = \begin{bmatrix} M_{11}(\omega) & M_{12}(\omega) \\ M_{21}(\omega) & M_{22}(\omega) \end{bmatrix} \begin{bmatrix} Q_N(\omega) \\ T_N(\omega) \end{bmatrix} \tag{6}$$

Putting aside, for the moment, the considerable computation associated with multiplying the N transfer matrices to determine the multilayer transfer matrix M, the solution for the heat pulse experiment can now be symbolically written; the computational issue is addressed shortly. For thermal pulse experiments for which it is appropriate to neglect radiative heat loss [10], the adiabatic condition $Q_N(\omega) = 0$ applies to the rear surface. Thus, using Eq. (6),

$$Q_0(\omega) = M_{12}(\omega)\, T_N(\omega) \qquad \text{or} \qquad T_N(\omega) = Q_0(\omega)/M_{12}(\omega) \tag{7}$$

For the case of an imposed heat flux on the front surface, e.g., the thermal pulse, adiabatic conditions otherwise holding on this surface as well, the

temperature transient on the rear surface is obtained using the inverse Fourier transform

$$T_N^0(t) = \frac{1}{2\pi} \int_{-\infty}^{\infty} T_N(\omega)\, e^{i\omega t}\, d\omega = \frac{1}{2\pi} \int_{-\infty}^{\infty} \frac{Q_0(\omega)}{M_{12}(\omega)}\, e^{i\omega t}\, d\omega \tag{8}$$

where $Q_0(\omega)$ is the Fourier transform of the imposed heat flux. For a thermal pulse that is a delta function in time and conveys total energy per unit area Q, neglecting radiative heat loss and using the symmetry of the integrand, Eq. (8) yields

$$T_N^0(t) = \frac{Q}{\pi} \operatorname{Re}\left[\int_0^{\infty} \frac{e^{i\omega t}}{M_{12}(\omega)}\, d\omega \right] \tag{9}$$

This is the temperature transient at the rear surface after a thermal pulse experiment that is sufficiently faster than the response time of the sample. Normalizing the *temperature transient* by the maximum *temperature excursion* ΔT, the ratio of pulse heat per unit area Q and sample specific heat per unit area c_A, gives a signal of unit amplitude

$$\frac{T_N(\infty) - T_N(0)}{Q/c_A} = 1 \tag{10}$$

Once normalized, the solution given in Eq. (9) has a single functional form independent of the total heat per area Q supplied by the heat pulse, a result that has been recognized previously by Parker et al. [11, 12] for homogeneous samples. Thus, neither accurate control nor measurement of the heat per unit area Q imparted to the sample is necessary. The experimental data need only be scaled so that the temperature transient has a unit amplitude and the functional form can be determined. Note that the normalized transform solution goes from $-\frac{1}{2}$ to $+\frac{1}{2}$, rather than from 0 to 1.

2.2. Simplification of the Integral Solution

The solution as presented in Eq. (9) is no more useful than most numerical schemes, as it still retains the complexity of the multilayer in the matrix multiplication required to determine $M_{12}(\omega)$. However, significant simplification is possible for periodic multilayer specimens. The first step in the simplification is accomplished by an eigenvector decomposition [13] of the matrix C, allowing it to be written in the form

$$C = S\, \Delta S^{-1} \tag{11}$$

The matrix Δ has the form

$$\Delta = \begin{bmatrix} \lambda_1 & 0 \\ 0 & \lambda_2 \end{bmatrix} \tag{12}$$

with diagonal elements λ_1 and λ_2 that are the eigenvalues of the transfer matrix C. The matrix S contains the eigenvectors of the transfer matrix C; the matrix S^{-1} is the inverse of S. The reason for expressing C in this way becomes clear when the multilayer transfer matrix M is evaluated

$$M = C^N = (S\Delta S^{-1})_1 (S\Delta S^{-1})_2 \cdots (S\Delta S^{-1})_N = S\Delta^N S^{-1} \tag{13}$$

where the subscripts $1 \cdots N$ merely indicate the repetition of the basis structure in the multilayer. The matrix algebra identities

$$S^{-1}S = \begin{bmatrix} 1 & 0 \\ 0 & 1 \end{bmatrix} \tag{14}$$

and

$$\Delta^N = \begin{bmatrix} \lambda_1^N & 0 \\ 0 & \lambda_2^N \end{bmatrix} \tag{15}$$

have been used to obtain the simplified expression at the right of Eq. (13). The elements of the Δ, S, and S^{-1} matrices can be easily determined for arbitrary matrix C. The N matrix multiplications required to determine the transfer matrix M are thus reduced to three matrix multiplications.

For a multilayer thermal barrier composed of alternating layers of materials A and B (Fig. 2), with an interface resistance ρ at each interface, the transfer matrix C of the repeat element is itself the product of four transfer matrices representing the two layers and an interface in front of each,

$$C = R \cdot A \cdot R \cdot B \tag{16}$$

The transfer matrices A and B have the same form as the transfer matrix τ introduced in Eq. (2), the elements given in Eq. (3); it is only necessary to substitute appropriate values for the thermal conductivity, thermal diffusivity, and thickness (κ, α, and L, respectively) of each layer.

The results of the linear algebra procedures described above are as follows. The transfer matrix C of the bilayer, determined by the matrix multiplication indicated in Eq. (16), is

$$C = \begin{bmatrix} C_{11} & C_{12} \\ C_{21} & C_{22} \end{bmatrix} \tag{17}$$

where

$$C_{11} = (\rho \cosh(\Delta_2) + \sinh(\Delta_2)/\gamma_2)\,\gamma_1 \sinh(\Delta_1) + \cosh(\Delta_1)\cosh(\Delta_2) \tag{18a}$$

$$C_{12} = (\cosh(\Delta_2) + \rho\gamma_2 \sinh(\Delta_2))\,\gamma_1 \sinh(\Delta_1) + \gamma_2 \sinh(\Delta_2)\cosh(\Delta_1) \tag{18b}$$

$$C_{21} = (\rho \cosh(\Delta_2) + \sinh(\Delta_2)/\gamma_2)(\cosh(\Delta_1) + \rho\gamma_1 \sinh(\Delta_1)) + \cosh(\Delta_2)(\rho \cosh(\Delta_1) + \sinh(\Delta_1)/\gamma_1) \tag{18c}$$

$$C_{22} = (\cosh(\Delta_1) + \rho\gamma_1 \sinh(\Delta_1))(\cosh(\Delta_2) + \rho\gamma_2 \sinh(\Delta_2)) + \gamma_2 \sinh(\Delta_2)(\rho \cosh(\Delta_1) + \sinh(\Delta_1)/\gamma_1) \tag{18d}$$

with

$$\Delta_j \equiv \sqrt{\frac{i\omega}{\alpha_j}}\, L_j \qquad \text{and} \qquad \gamma_j \equiv \sqrt{\frac{i\omega}{\alpha_j}}\, \kappa_j \qquad (j = 1, 2) \tag{19}$$

The conductivity, diffusivity, and thickness of layers A and B are indexed using subscript 1 and 2, respectively. The eigenvalues of C are obtained from the solution of a quadratic. Representing the discriminant by

$$\Phi = \sqrt{C_{11}^2 + C_{22}^2 - 2C_{11}C_{22} + 4C_{12}C_{21}} \tag{20}$$

the expressions for the eigenvalues are

$$\begin{aligned} \lambda_1 &= (C_{11} + C_{22} + \Phi)/2 \\ \lambda_2 &= (C_{11} + C_{22} - \Phi)/2 \end{aligned} \tag{21}$$

The solution for the rear surface temperature with N bilayers of the form Eq. (16) is given by

$$T_N^0(t) = \frac{Q}{2\pi} \int_{-\infty}^{\infty} \frac{\Phi e^{i\omega t}}{C_{12}(\lambda_1^N - \lambda_2^N)}\, d\omega \tag{22}$$

after the ideal thermal pulse, energy per unit area Q, has been applied to the front surface. The final step is to normalize the solution by the maximum rear surface temperature excursion Q/c_A. Because the specific heat per unit volume of each layer is given by the ratio of its conductivity and diffusivity, κ/α, the specific heat per unit area of the N bilayers is

$$c_A = N\left(L_1 \frac{\kappa_1}{\alpha_1} + L_2 \frac{\kappa_2}{\alpha_2}\right) \tag{23}$$

The normalized rear surface temperature transient, value -0.5 at $t=0$ and value $+0.5$ as $t \to \infty$, is therefore

$$\frac{T_N^0(t)}{Q/c_A} = \frac{1}{\pi N(L_1\kappa_1/\alpha_1 + L_2\kappa_2/\alpha_2} \operatorname{Re}\left[\int_0^{\prime} \frac{\Phi e^{i\omega t}}{C_{12}(\lambda_1^N - \lambda_2^N)}\, d\omega\right] \tag{24}$$

where the symmetry of the solution has been used to reduce the integral bounds.

Though it is still necessary to evaluate the integral solution numerically, the solution is computationally simpler than discretization of the equations governing heat transfer and time stepping. Unlike discretized solutions, the temperature need only be evaluated at the time or times of interest and the computational complexity is independent of the number of bilayers N in the film. The solution is valid until thermal losses become nonnegligible.

2.3. Multilayer with a Capping Layer on a Substrate

The integral solution as described thus far is not sufficient for analysis of the experiments presented here because the multilayers being studied, for reasons explained in Section 3.1, are not freestanding. Accounting for a substrate, the capping layer over the multilayer and the interface between the multilayer and the capping layer, the transfer matrix is

$$M^* = D \cdot M \cdot R \cdot E \tag{25}$$

where the matrix M is the transfer matrix for the periodic multilayer determined in Eq. (13), R is for the interface resistance between the multilayer and capping layer, its form given in Eq. (4), and D and E are the transfer matrices for the substrate and capping layer, respectively; their form is that of the transfer matrix τ given in Eq. (3) with the appropriate conductivities, diffusivities, and thicknesses substituted. The equation describing the normalized temperature transient on the rear (capping surface) after the thermal pulse is applied to the substrate surface at $t=0$ is given by

$$\frac{T_N^0(t)}{Q/c_A^*} = \frac{1}{\pi c_A^*} \operatorname{Re}\left[\int_0^{\prime} \frac{e^{i\omega t}}{M_{12}^*}\, d\omega\right] \tag{26}$$

where

$$M_{12}^* = \sum_{i=1}^{2} \sum_{j=1}^{2} \sum_{k=1}^{2} D_{1i} M_{ij} R_{jk} E_{k2} \tag{27}$$

and the specific heat per unit area of multilayer with substrate and cap is given by

$$c_A^* = N\left(L_1\frac{\kappa_1}{\alpha_1} + L_2\frac{\kappa_2}{\alpha_2}\right) + L_D\frac{\kappa_D}{\alpha_D} + L_E\frac{\kappa_E}{\alpha_E} \tag{28}$$

The subscripts D and E indicate properties of the substrate and capping layers, respectively.

3. EXPERIMENTAL PROCEDURE

3.1. Samples

Thermal pulse experiments were performed on five molybdenum (99.95 wt%) samples, 12 mm in diameter and 199 to 241 μm thick, to ascertain the reliability of the measurement system. The samples were cut and ground from sheet stock and polished. The two faces of the samples were optically flat and deviated from parallel by less than 1 μm over the 3-mm-diameter area viewed by the photodiode.

Thermal pulse experiments were performed on five samples of iron/copper multilayer on molybdenum to study thermal transport in multilayers. The multilayer samples studied were deposited using electron beam evaporation sources. The deposition rate was approximately 1 nm $\cdot$ s^{-1} in a low 10^{-4}-Pa (10^{-6}-Torr) vacuum with the substrates placed on an uncooled, rotating platen over the sources. Deposition was monitored using a quartz crystal oscillator positioned at the center of the rotating platen. The multilayers were fabricated with 10 bilayers, each nominally 2/3-μm copper and 4/3-μm iron. The charges used for the deposition were 99.99 wt% copper and 99.98 wt% iron. These materials were chosen because they are immiscible and do not form intermetallics. The layer thicknesses were chosen because they were thick enough to ensure layer integrity during the course of the experiments [14]. The iron layers were thicker to capitalize on iron's low thermal diffusivity.

It was found that free-standing 20-μm-thick multilayer samples vibrated after the thermal pulse; the oscillations in signal intensity were large enough to preclude acquisition of meaningful data. Because the available deposition facilities did not allow convenient deposition of thicker films, the multilayers were deposited on substrates. As the thermal transport properties assumed for the substrate could unintentionally affect the determined values of the thin film thermal transport properties, the 75-μm molybdenum (99.9 wt%) foil substrates used were the thinnest for which measurements without significant vibrations were achieved. All of the

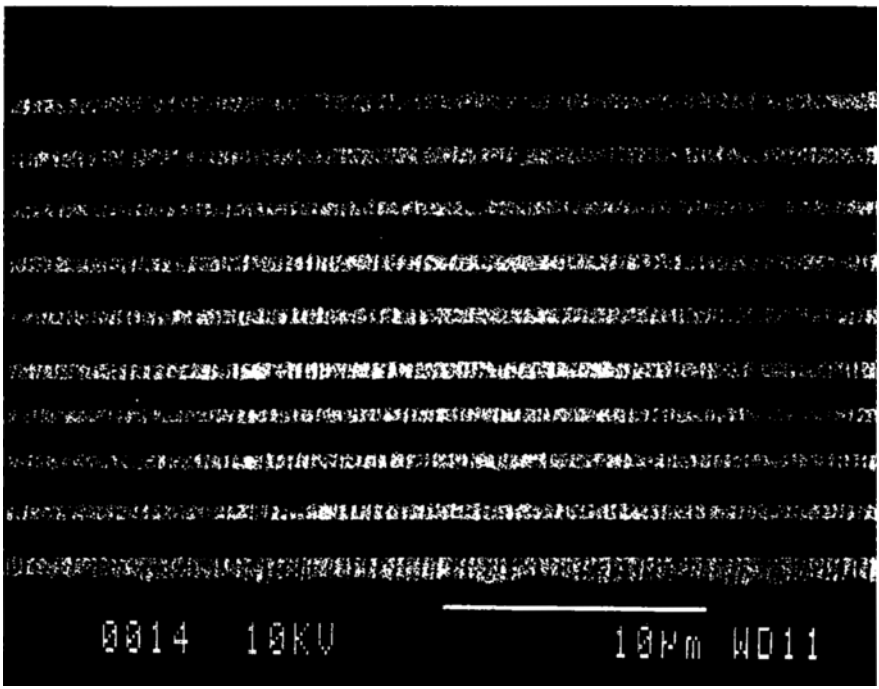

Fig. 3. A free-standing piece of the iron/copper multilayer in the as-deposited state, viewed in cross section by scanning electron microscope. Thickness variation of the first (bottom) layers was associated with a faulty thickness monitor during deposition. The layer thicknesses, 1.29 μm of iron (dark) and 0.59 μm of copper, are therefore the average thicknesses of each type of layer.

samples studied were 6.4 mm in diameter and came from a single piece of coated foil. A micrograph of an as-deposited sample viewed in cross section, obtained using a scanning electron microscope, is shown in Fig. 3. Layer thicknesses and bulk properties [15, 16] of the three metals in the multilayer samples are given in Table I for use in the integral solution.

3.2. Measurement Technique

Thermal pulse experiments were conducted using a modified version of a laser pulse system described elsewhere [17]. The modifications include addition of a Q-switch for the pulsed laser heating source, to shorten the pulse duration from about 1 ms to less than 50 ns, and redesign of the differential gain electronics, both required to work with the submillisecond duration of the thermal pulse experiments. In addition, the silicon photodetector used to monitor the radiance of the back surface of the

Table I. Bulk Transport Properties at 1200 K and Dimensions for Constituent Materials of Iron/Copper Multilayer on Molybdenum[a]

Material	Thermal diffusivity ($cm^2 \cdot s^{-1}$)	Thermal conductivity ($W \cdot cm^{-1} \cdot s^{-1}$)	Layer(s) thickness (μm)
Copper	0.838(±6%)	3.42(±3–5%)	0.59(±2%)
Iron	0.0605(±4%)	0.282(±3–8%)	1.29(±2%)
Molybdenum	0.339(±6%)	1.05(±4–10%)	75(±2%)

[a] Thermal diffusivities and thermal conductivities of bulk copper, iron, and molybdenum are from Refs. 15 and 16. Layer thicknesses, average for copper and iron, as determined by SEM (Fig. 3) of samples viewed in cross section.

sample was replaced with an InGaAs photodetector to improve the signal-to-noise ratio at lower temperatures (<1250 K). The low temperatures were necessary to minimize destructive grain boundary grooving in the sample [14] and to retard the formation of iron–molybdenum intermetallic at the multilayer/substrate interface. The remainder of the system was unchanged. A laser pulse was delivered to one side of the sample maintained at a quasi-steady-state high temperature in a 10^{-4}-Pa (10^{-6}-Torr) vacuum. The radiance of a circular region (less than 3.2 mm in diameter) on the other side of the sample, after subtraction of the baseline, amplification, and recording at a 2-MHz rate with a digital oscilloscope, yielded the temperature transient. The temperature of the sample before the laser pulse was measured with an optical pyrometer aimed at the blackbody cavity of the sample holder [17].

To reduce vibrations associated with the laser pulse, the sample was sandwiched between two molybdenum annuli: inner diameter 4.8 mm above the sample (substrate side) and inner diameter 3.2 mm below the sample (multilayer side). The laser pulse was administered to the substrate side in all experiments; the temperature transient was monitored on the multilayer side. The annulus on the substrate side restricted the irradiated area (otherwise 6.4-mm diameter). Radiative losses should be insignificant during the brief (<1-ms) experiments [10]. Minimal long-term cooling of the rear surface after the initial temperature excursion indicated that conditions were in fact nearly adiabatic. Therefore, for the 100-μm-thick specimens, irradiation of the 4.8-mm-diameter region above gave reasonably one-dimensional heat flow within the monitored region (diameter, <3.2 mm), and thermal contact of the smooth sample (<1-μm rms on both sides) with the machined annuli did not play a significant role.

4. MEASUREMENTS

4.1. Molybdenum

Experiments were conducted on five pure molybdenum samples. Each value of thermal diffusivity was determined by least-squares fitting of Parker's solution [12] to the normalized transient radiance data in the vertical range 0.2 to 0.8. The thermal diffusivity results on the five molybdenum samples, of which three were studied twice, are presented in Fig. 4 in addition to recommended values from Ref. 16. The data fall within the $\pm 6\%$ uncertainty of the recommended curve.

4.2. Iron/Copper Multilayer on Molybdenum Substrates

Experiments were conducted on five iron/copper multilayer samples that came from the same piece of coated molybdenum and had essentially identical layer dimensions. Samples were brought to a quasi-steady-state temperature in approximately 15 min, after which up to 20 laser pulses were applied at approximately 2-min intervals. In an effort to minimize reactions at the substrate/coating interface, visible in Fig. 5, no sample was exposed to the high temperatures for more than 50 min.

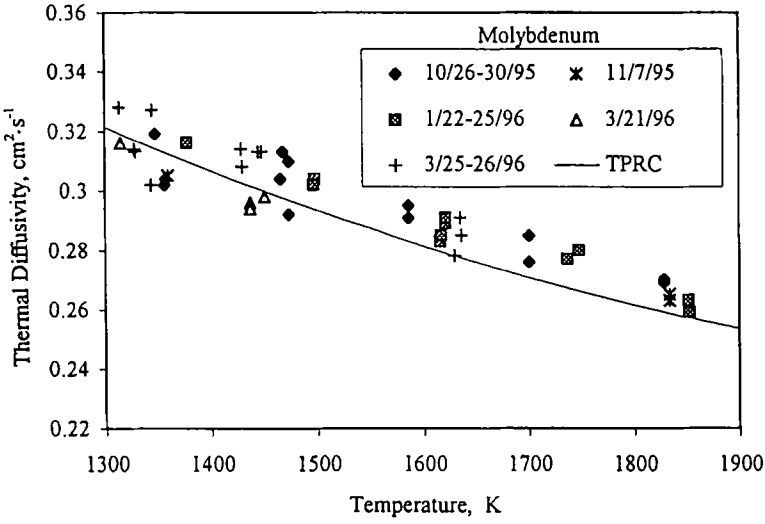

Fig. 4. The thermal diffusivity of molybdenum (99.95 wt%) samples as determined by pulse heating experiments. The curve represents the recommended values by TPRC [16].

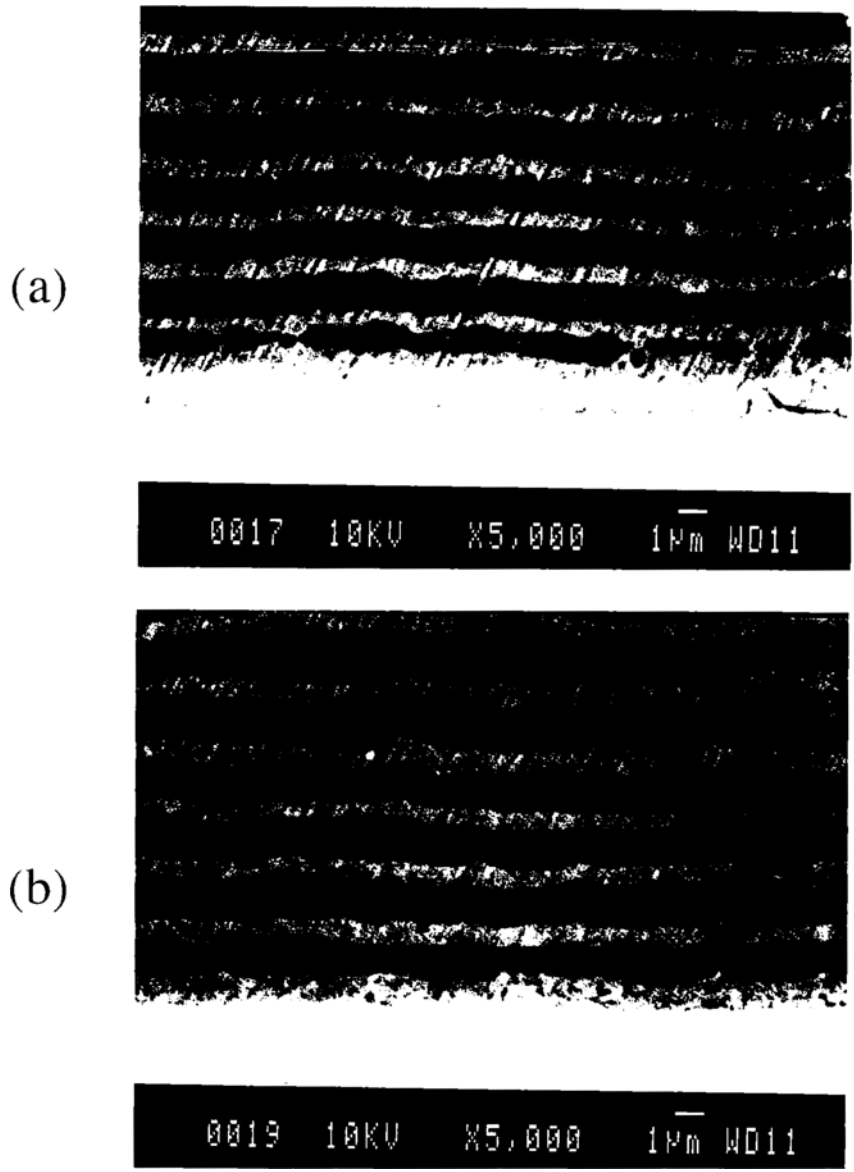

Fig. 5. Micrographs of the iron/copper multilayer on molybdenum samples after pulse heating experiments at two different temperature ranges. The dark spots are pores. (a) Higher temperature: Formation of intermetallic at the multilayer/substrate interface and depletion of the first (bottom) iron layer (dark) are substantial. (b) Lower temperature: Depletion of the first iron layer and intermetallic formation are not evident. The samples are viewed in cross section by a scanning electron microscope.

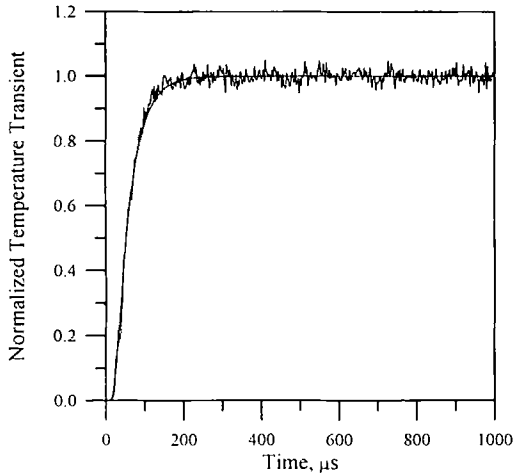

Fig. 6. Temperature transient (normalized) at the back surface of an iron/copper multilayer on molybdenum sample in a typical experiment. The data have been smoothed: each group of five data points replaced by a single value, at the middle time, determined by a quadratic fit. The ambient temperature of this experiment was 1237 K and the temperature transient 4.3 K. The transient time $t_{1/2}$ is 51.8 μs. Though not shown, data were acquired over 4 ms and manifested insignificant cooling in that time.

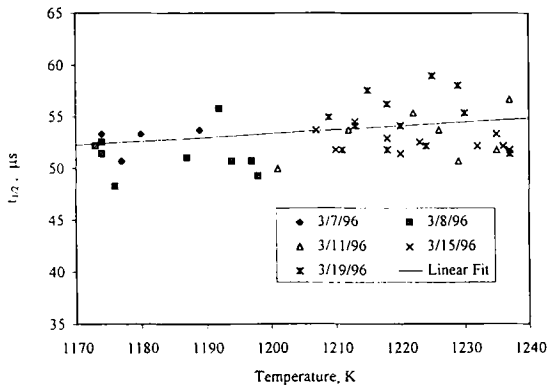

Fig. 7. The dependence of the transient time $t_{1/2}$ on the temperature of the iron/copper multilayer on molybdenum samples.

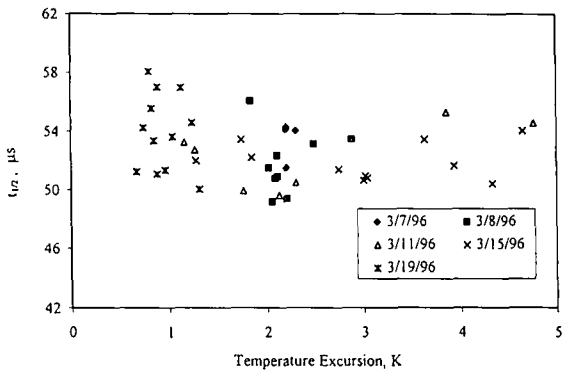

Fig. 8. The dependence of the transient time $t_{1/2}$ on the temperature excursion ΔT of the iron/copper multilayer on molybdenum samples. Values have been adjusted to 1200 K having accounted for different sample temperatures using the temperature dependence indicated in Fig. 7.

Figure 6 shows one thermal pulse experiment conducted on a sample of iron/copper multilayer on molybdenum. The temperature excursion of the back side is 4.3 K and the measurement temperature 1237 K. The time required for the temperature transient to reach half its maximum value, $t_{1/2}$, determined by least-squares fitting of Parker's [12] solution for a *homogeneous* material to the data in the vertical range 0.2 to 0.8, was 51.8 μs. The best-fit transient obtained from Parker's solution for homogeneous materials is also shown. All of the experimental results are summarized in Figs. 7 and 8. Figure 7 shows the observed $t_{1/2}$ dependence on sample temperature. Figure 8 shows the same data, extrapolated to 1200 K using the linear temperature dependence shown in Fig. 7, as a function of the temperature excursion ΔT.

The $t_{1/2}$ values in Figs. 7 and 8 were determined by least-squares fitting of Parker's curve for homogeneous material to the data in the vertical range 0.2 to 0.8 because its shape is very similar to that of the full multilayer solution. Because of the significant noise in the data, this should yield a more accurate value for $t_{1/2}$ than a straight-line fit to limited data near the 0.5 crossing. The $t_{1/2}$ value is used both because it uniquely determines the Parker curve and because it is commonly used for analyzing results from homogeneous samples.

5. RESULTS

Baseline and maximum temperatures, i.e., radiant intensities converted to voltages by the photodetector and amplification electronics, were

required for scaling the data obtained from experiments on the pure molybdenum and multilayer coated molybdenum. In both cases, the average intensity during the 0.6 ms between activation of the laser lamp and activation of the Q-switch that induced lasing was equated to the baseline. The average intensity from 1 to 4 ms after lasing was equated to the maximum for the molybdenum samples, 0.4 to 1 ms for the multilayer samples. After scaling to unity, the data were numerically compared to the Parker solution; the value of $t_{1/2}$ that minimized the least-squares difference for times when the Parker solution was within the vertical range 0.2 to 0.8 is the experimental value used in this paper.

Of the thermal diffusivity values obtained from experiments on the five molybdenum samples included in this work, the results of about 40% of the experiments are shown in Fig. 4. Of the $t_{1/2}$ values obtained from the five multilayer/substrate samples, 60% appear in Figs. 7 and 8.

The remaining experiments are not presented in this work because of flawed data that might have resulted from (a) large vibrations of the sample, (b) temperature decay caused by lateral heat flow when the monitored location was accidentally near the edge of the region heated by the laser pulse, and (c) a nonsteady baseline signal possibly associated with laser prefire or electronic noise. To detect drift of the baseline, an additional $t_{1/2}$ value was obtained by equating the baseline signal to the average intensity during the 200 μs (instead of the 400 μs used originally) immediately prior to lasing. To detect heat loss from the Mo samples, an additional $t_{1/2}$ value was obtained by equating the maximum signal to the average intensity during the period 1 to 2 ms after lasing instead of the 1 to 4 ms used originally; for the multilayer samples, 0.4 to 1.0 ms was replaced by 0.3 to 0.6 ms. All the experiments for which either of these two values differed from the original value by 2% or more were discarded. If both values differed from the original value by less than 1%, the experiment was kept. If either or both of these values differed by 1 to 2% from the original value, the overall data curve was judged more critically for deviations from the Parker shape, such as those arising from vibrations, and either kept or discarded on this basis.

Because the thermal transport properties generally depend on temperature T, a measurement error is expected if the temperature excursion ΔT is excessively large. This occurs because, for the pulse duration used in these experiments, the very thin region at the sample surface that originally absorbs the heat pulse [7] has a temperature rise of the order of 100 times the long-term temperature excursion. Temperature dependence of transport properties thus becomes an issue. The larger the heat absorbed, the longer (temporally) and larger (spatially) a region with temperature excursion greater than a given value will exist during the course of equilibration, and

Table II. Comparison of Experimental and Theoretical Results on Iron/Copper Multilayer on Molybdenum at 1200 K

Source	$t_{1/2}$ (μs)
Experiment (from fit at 1200 K)	53.4 ± 0.8
Integral solution (properties from Table I): $p = 0$ K · cm^2 · W^{-1}	49.3
Integral solution (properties from Table I): $p = 2 \times 10^{-5}$ K · cm^2 · W^{-1}	50.6
$\kappa_{avg} = 1/[1/\kappa]$ and $\alpha_{avg} = 1/([\kappa/\alpha][1/\kappa])$[a]	49.5
$\kappa_{avg} = [\kappa]$ and $\alpha_{avg} = [\alpha]$[a]	38.3
$\kappa_{avg} = 1/[1/\kappa]$ and $\alpha_{avg} = [\alpha]$[a]	32.6

[a] The multilayer has been modeled as homogeneous with κ_{avg} and α_{avg} determined from the thickness averages, indicated by brackets, of the quantities indicated in Table I. The properties of the molybdenum substrate are those in Table I. Note that the ratio κ/α is the specific heat per unit volume.

the larger the error it will introduce. The data shown in Figs. 7 and 8 had thermal excursions of 5 K or less because larger values had a clear effect on the $t_{1/2}$ values observed and thus were not meaningful. The magnitude of the thermal transient had an insignificant effect on the $t_{1/2}$ value for ΔT less than 5 K (Fig. 8) and is therefore ignored. A least-squares fit of the $t_{1/2}$ data (Fig. 7) to the form $t_{1/2} = A + B(T - 1200)$ gives $A = 53.4 \pm 0.8\,\mu$s and $B = 0.037 \pm 0.02\,\mu$s · K^{-1}. Though the sign (positive) of the temperature dependence is clear, its value is not.

The $t_{1/2}$ values obtained experimentally on the iron/copper on molybdenum samples are compared with several predicted values in Table II. Predicted values include those obtained from the integral solution, Eq. (26), with bulk properties as listed in Table I. Other values, obtained from the integral solution with the thermal conductivities and thermal diffusivities of the layers in the coating replaced by various forms of thickness averaged iron and copper properties, are included for comparison as such averaging is frequently done to model these materials.

6. DISCUSSION

Using the thermal diffusivity value given in Table I, the molybdenum substrate alone would yield $t_{1/2} = 23.0\,\mu$s in a thermal pulse experiment. The effect of the iron/copper multilayer coating is clear in the experimental data. However, the 8% difference between the $t_{1/2}$ value predicted by the integral solution using bulk material properties and the experimental value, both shown in Table II, is large. Thickness averaging, indicated by square brackets, of the thermophysical properties results in errors manifesting as

disagreement with the integral solution. The disagreement for $\kappa_{avg} = [\kappa]$ and $\alpha_{avg} = [\alpha]$ is not a surprise, as averaging of the conductivity is not correct even for steady-state heat transfer. Using $\kappa_{avg} = 1/[1/\kappa]$ and $\alpha_{avg} = [\alpha]$, though correct for steady-state heat tansfer, is clearly incorrect for modeling of transients. Only averaging of $1/\kappa$ and κ/α is appropriate for approximating the average properties of the sample. If the multilayer material is composed of sufficiently many bilayers then, *absent an interface resistance*, the approximate solution with $\kappa_{avg} \equiv 1/[1/\kappa]$ and $\alpha_{avg} \equiv 1/([\kappa/\alpha)][1/\kappa])$ will converge to the integral solution.

The interface resistance, though introduced in the development of the integral solution, has been set to zero in the modeling of these samples. For interface resistance $\rho = 2 \times 10^{-5}\ \mathrm{cm^2 \cdot K \cdot W^{-1}}$, Fig. 9 shows the predicted effect on the thermal transient of increasing the number of interfaces within a given thickness of coating, i.e., reducing the bilayer thickness. The value of interface resistance used is representative of values obtained from other metal/metal multilayer systems [8]. Based on this value, as shown in Table II, the interface resistance would account for approximately one-third

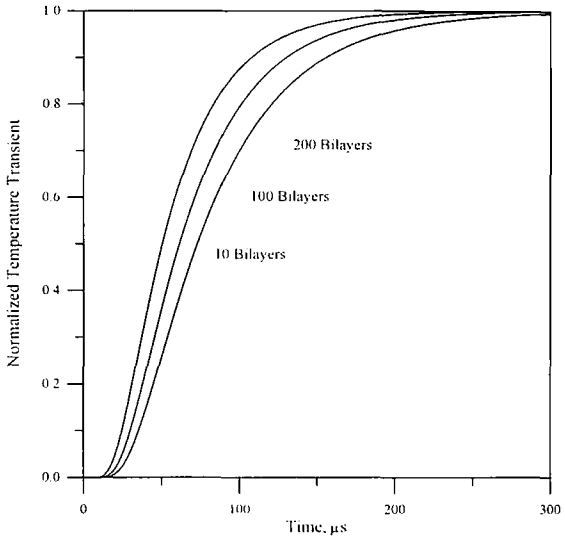

Fig. 9. Calculations of temperature transients of iron/copper multilayer on molybdenum samples where the number of bilayers is varied, the interface resistance is $2 \times 10^{-5}\ \mathrm{cm^2 \cdot K \cdot W^{-1}}$, and bulk properties are from Table I. Total thicknesses of iron, copper, and molybdenum substrate are fixed at 12.9, 5.9, and 75 μm, respectively. The curves were obtained from the integral solution of the heat transfer equation.

(1.3 μs) of the 8% (4.1 μs) difference between the observed and the predicted values of $t_{1/2}$.

The discrepancy between the transient time $t_{1/2}$ predicted by the integral and the measured value is larger than the $\pm 5\%$ standard deviation of the measurements (Fig. 8). The relatively large standard deviation of the data is associated with the low signal-to-noise ratio at the low temperatures necessitated by the low melting point of the samples (Fig. 7). The discrepancy is also somewhat larger than the uncertainties in the bulk properties, shown in Table I, that were used in the integral solution [15, 16].

Perhaps of greatest concern are the voids evident in specimens held at elevated temperatures (Fig. 5). The voids are likely the result of annealing out excess defects, e.g., grain boundaries, incorporated into the specimen during deposition. The voids would reduce thermal transport through that region of the sample, decreasing thermal conductivity and increasing $t_{1/2}$, consistent with the discrepancy. It should be noted that if the voids are distributed throughout the sample, they would also decrease the specific heat per unit volume, partly offsetting the previous effect.

An additional concern is the reacted region at the substrate/coating interface seen in Fig. 5. One of the samples studied, shown in Fig. 5a, was held for 50 min at temperatures between 1209 and 1237 K. During the diffusion transient the interface may contain both the equilibrium phases Fe_2Mo and Fe_3Mo_2 below 1200 K but should contain only Fe_3Mo_2 above 1200 K [18]. It is expected that the reaction layer formed by diffusion of iron from the first iron layer through the first copper layer to the molybdenum substrate; note the depletion of the first iron layer. The second sample studied, shown in Fig. 5b, held for 35 min between 1171 and 1189 K, has a thinner reacted layer consistent with the lower temperature and shorter duration. Both the reacted region and the interdiffusion of the iron and copper might retard heat flow, consistent with the observed discrepancy. However, no clear trend of $t_{1/2}$ during the experiments was noted, inconsistent with a connection between the thickening reacted layer and the discrepancy between measurement and prediction.

Though pure iron changes from a bcc to an fcc crystal structure at 1185 K [19], copper in solution can lower this value to 1123 K [19]. However, the difference in $t_{1/2}$ associated with the phase change is anticipated to be less than the experimental uncertainty. Analysis of steady-state heat transfer across the sample indicates that the sample temperature may be 11 K lower than the temperature of the specimen holder measured by the pyrometer [17]. Also, increasing temperatures, 1 to 2 $K \cdot min^{-1}$, indicated that thermal equilibrium was not reached in most experiments, a result of the desire to minimize reaction at the interface, i.e., duration

at high temperature. Nonetheless it is believed that thermal equilibrium was reasonably good because, for small temperature excursions, an approximately linear relationship existed between the radiances measured by the pyrometer and the InGaAs photodiode.

7. CONCLUSION

An exact integral solution to the time-dependent heat transfer equation for periodic multilayers with an arbitrary number of repeat units N has been developed. This integral solution has been used as a tool to analyze the transient associated with thermal pulse experiments on multilayer coated substrates. In particular, comparison of the predicted transient time $t_{1/2}$ based on bulk thermal transport properties with the results of experiments conducted on iron/copper multilayers on molybdenum substrates has yielded an 8% (4-μs) difference. Possible explanations for the discrepancy, including voids, reaction layer, and Fe phase change, have been noted. Furthermore, comparison with results predicted by assuming the multilayer to be a homogeneous material with thermal transport properties determined by thickness averaging (quantities given in brackets) the properties of the constituent layers has demonstrated that only the choice $\kappa_{avg} \equiv 1/[1/\kappa]$ and $\alpha_{avg} \equiv 1/([\kappa/\alpha)][1/\kappa])$ is acceptable.

For the samples studied, the effect of interface resistance is expected to be small. Films with higher densities of interfaces, i.e., thinner layers, were not pursued in this work because the layered structure broke down at these temperatures. It is anticipated that modifications of the measurement system to lower the range of operating temperatures will, with the integral solution presented in this work, permit interface resistances to be determined from the results of future pulsed laser heating experiments on samples with higher densities of interfaces.

REFERENCES

1. R. E. Taylor and K. D. Maglić, in *Compendium of Thermophysical Property Measurement Methods 1: Survey of Measurement Techniques*, K. D. Maglić, A. Cezairliyan, and V. E. Peletsky, eds. (Plenum, New York, 1984), pp. 305–336.
2. K. D. Maglić and R. E. Taylor, in *Compendium of Thermophysical Property Measurement Methods 2: Recommended Measurement Techniques and Practices*, K. D. Maglić, A. Cezairliyan, and V. E. Peletsky, eds. (Plenum, New York, 1992), pp. 281–314.
3. J. Albers, *IEEE Trans. Compon. Pack. Manuf. Tech.* **A18**:31 (1995).
4. M. D. Mikhailov, M. N. Özisik, and N. L. Vulchanov, *Int. J. Heat Mass Transfer.* **26**:1131 (1983).
5. A. G. Kokkas, *IEEE Trans. Elect. Dev.* **ED-21**:674 (1974).
6. S. C. Choo, M. S. Leong, and K. L. Kuan, *Solid-State Elect.* **19**:561 (1976).
7. C. A. Paddock and G. L. Eesley, *J. Appl. Phys.* **60**:285 (1986).

8. B. M. Clemens, G. L. Eesley, and C. A. Paddock, *Phys. Rev. B* **37**:1085 (1988).
9. H. S. Carlslaw and J. C. Jaeger, *Conduction of Heat in Solids*, 2nd ed. (Clarendon Press, Oxford, 1959), pp. 109–112.
10. D. Josell, J. A. Warren, and A. Cezairliyan, *J. Appl. Phys.* **78**:6867 (1995).
11. R. L. Rudkin, R. J. Jenkins, and W. J. Parker, *Rev. Sci. Instr.* **33**:21 (1962).
12. W. J. Parker, R. J. Jenkins, C. P. Butler, and G. L. Abbott, *J. Appl. Phys.* **32**:1679 (1961).
13. E. Isaacson and H. B. Keller, *Analysis of Numerical Methods* (Wiley, New York, 1966), Chap. 4.
14. D. Josell and F. Spaepen, *Acta Metall. Mater.* **41**:3017 (1993).
15. Y. S. Touloukian, R. W. Powell, C. Y. Ho, and P. G. Klemens, *Thermophysical Properties of Matter, Vol. 1* (Plenum, New York, 1970).
16. Y. S. Touloukian, R. W. Powell, C. Y. Ho, and M. C. Nicolaou, *Thermophysical Properties of Matter, Vol. 10* (Plenum, New York, 1973).
17. A. Cezairliyan, T. Baba, and R. Taylor, *Int. J. Thermophys.* **15**:317 (1994).
18. P. Villars, A. Prince, and H. Okamoto, *Handbook of Ternary Alloy Phase Diagrams, Vol. 7* (ASM International, Materials Park, OH, 1995), pp. 9350–9356.
19. T. B. Massalski, H. Okamoto, P. R. Subramanian, and L. Kacprzak, *Binary Alloy Phase Diagrams, Vol. 2*, 2nd ed. (ASM International, Materials Park, OH, 1990), pp. 1408–1409.

Printed in Belgium